UDC 549.651:5[illegible].8.013

THE QUENCHING OF MINERAL TRANSFORMATIONS AS EXEMPLIFIED BY ALKALI FELDSPAR ORDERING*

E. E. Senderov, L. M. Truskinovskiy and Ye. A. Mitina

Vernadskiy Institute of Geochemistry and Analytical Chemistry, USSR Academy of Sciences

Subsolidus transformations under nonisothermal conditions have been simulated not on the basis of *TTT* diagrams but by integrating the kinetic equations together with the heat-transport equation. Measurements of Al-Si ordering in alkali feldspars have been used in determining the quenching conditions in a particular system. We have taken into consideration the dependence of the equilibrium and kinetic parameters on temperature, pressure and composition and the influence of water pressure on grain size on the ordering rate constant. Variation in the cooling rate allowed us to examine the ordering process under various cooling conditions. Differences are noted between the quenched and equilibrium degrees of transformation, and studies have been made on the discrepancies between the quenched degree of order and the quenching conditions derived by the proposed method and by means of *TTT* diagrams.

It is becoming increasingly obvious that equilibrium is often not attained in a geochemical system and that kinetic features control its state. Research on reaction kinetics not only enables us to characterize the evolving phase relationships but also to explain grain zonation, rock textures, and so on. Kinetic analysis is a necessary step in describing processes within the planet and is the basis of geospeedometry. A study of reaction kinetics must thus be a basic aspect of geochemistry [1-3].

An important step in the study of the kinetics of reactions is the relation between reaction rates and the rates of change in the external parameters T, P and μ, as well as the transport rates of the reacting components. This enables us to determine when equilibrium is attained in the natural system, and if it is not, how far the observed phase relationships deviate from equilibrium ones. Kinetic studies may in particular be used to examine the conditions of quenching of mineral transformations.

Reaction rates are low at low temperatures such as in diagenesis. Equilibrium may not be attained, although the reaction may continue under constant conditions for geologically significant periods. When igneous rocks cool or when magmas and xenoliths are transported from a deep site to upper parts of the crust, the extent of reaction should be controlled by the rate at which external conditions change. Thus one estimates the temperatures and pressures at various stages in rock emplacement by the use of geothermometers and geobarometers would be impossible without careful research on how mineral reactions

*Translated from Geokhimiya, No. 1, pp. 121-134, 1991.

ISSN0016-7029/90/0008-0110$7.50/0
© 1991 Scripta Technca, Inc.

track changing conditions and when the reactions are quenched. Quenching studies form the basis of geospeedometers, which enable us to use data on the extent of reaction to estimate rates of change in conditions.

There are various categories of reaction: crystallization and recrystallization, pseudomorphous replacement and polymorphic transitions, intercrystallite and intracrystallite ion or isotope exchange, structural transformations associated with ordering, and so on. A feature of the description of nonequilibrium states is that the Gibbs energy during the reaction is dependent not only on the standard parameters T, P and composition (X_j, molar fractions of the components, $j = 1, 2, \ldots, n$) but also on parameters characterizing the completeness of reaction (ξ_a, $a = 1, 2, \ldots k$): $G = G(T, P, X_1, \ldots, X_n, \xi_1, \ldots \xi_k)$.

The independent internal parameters ξ_a may be taken as the molar fractions of the phases, the proportions of the components or isotopes in the coexisting phases, the proportions of the different types of atoms in positions within a single phase (degree of ordering), and so on. At equilibrium, G should have reached a minimum, so the equilibrium values of $\xi_a = \xi^*(P, T, X_j)$ are defined by

$$\partial G/\partial \xi_a|_{\xi^*} = 0.$$

The linear thermodynamics of irreversible processes [4] indicates that a simple kinetic equation describing the relaxation in a system having one degree of freedom towards equilibrium is

$$\frac{d\xi}{d\tau} = -k\frac{\partial G}{\partial \xi}, \qquad (1)$$

in which $k > 0$ is the kinetic coefficient, while $\partial G/\partial \xi$ characterizes the driving force and is defined by equilibrium-thermodynamic methods. The closeness of k to zero at sufficiently small T causes quenching, although the different degrees of freedom may be quenched at different temperatures.

Here we consider a method of estimating quenching conditions. As an example we will use the Al-Si ordering in alkali feldspars. The usual approach is based on time-temperature-transformation (TTT) diagrams. Here we propose a rigorous solution obtained by numerical integration. The method of defining the conditions of quenching that were developed and the relationships between the quenched degree of order and the transformation parameters that were found with its help indicate the effectiveness of using the feldspars are effective for solving problems of geospeedometry as cooling rate indicators.

SOLID-STATE REACTIONS UNDER NONISOTHERMAL CONDITIONS

Analysis TTT diagrams is the most familiar method of examining the nonisothermal kinetics and quenching conditions of solid-state reactions. Figure 1 shows the principles of constructing TTT diagrams. One uses kinetic curves from isothermal experiments, i.e., functions $\xi = \xi(T, \tau, \xi_0)$, in which $\xi_0 = \xi(T, \tau = 0)$ is the initial value of ξ, which characterizes the degree of completion of reaction and τ is time reckoned from the start of the experiment. To construct a TTT diagram one needs to draw contours for $\xi(T, \tau, \xi_0)$ (transformation) on the temperature-time T-τ plane. Let T^* be the equilibrium temperature corresponding to ξ_0, i.e., $\xi_0 = \xi(T^*, \tau = \infty)$. Then (1) shows that the rate $d\xi/d\tau$ is maximal for a certain supercooling T^*-T, which governs the specific form of the TTT diagram (Fig. 2).

To analyze the reaction during cooling, a curve is superimposed on the diagram that describes the temperature change with time. The intersections between the cooling curves and the ξ lines define the sequence of changes in the structural state. Figure 2 shows that ξ as a function of τ initially increases along a typical cooling curve but then passes through a maximum. The latter, which corresponds to the point where the cooling curve is tangential to some $\xi(T, \tau)$ line, is usually taken as the instant of quenching [6-9].

There is an element of incorrect approach in using these diagrams to determine quenching conditions and ξ during cooling because the ξ = constant curves are derived from isothermal kinetics, whereas the process is not isothermal, as

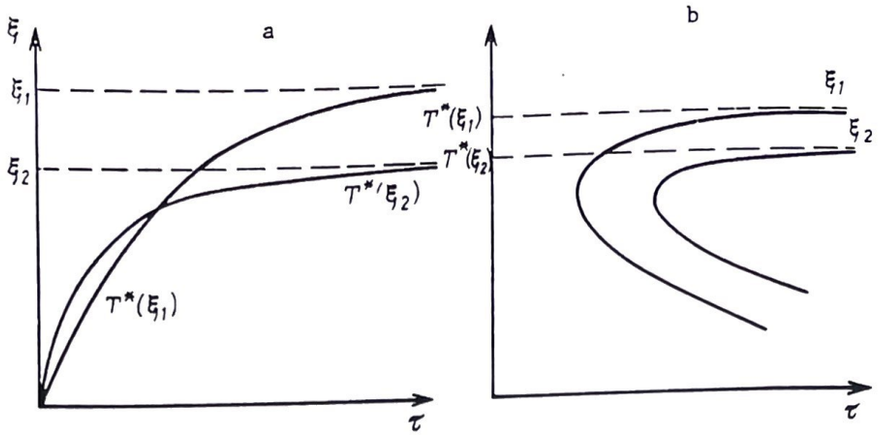

Fig. 1. *TTT* diagram construction: a) kinetic isotherms of a conversion characterized by temperature dependence of the equilibrium constant (ionic, isotope exchange, ordering, etc.); b) levels of the degree of conversion for the case shown in Fig. 1a.

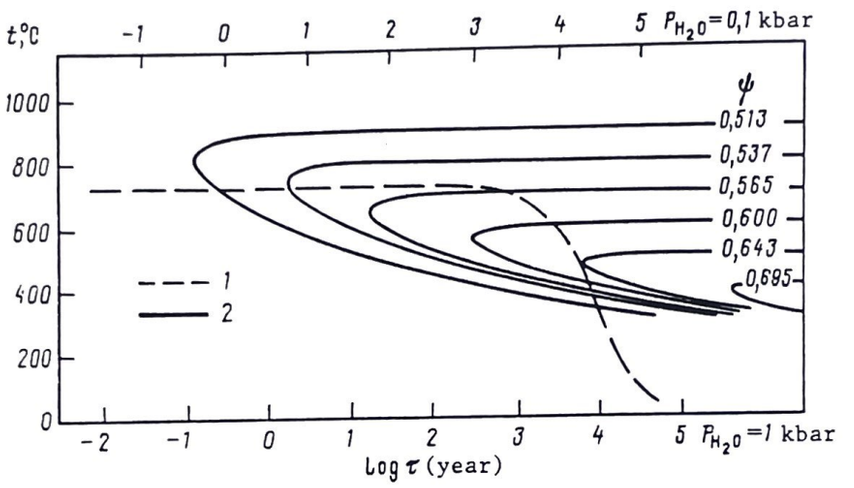

Fig. 2. *TTT* sanidine ordering diagram for X_{Or} = 0.7 constructed on the assumption that the structural state at the initial instant when $T = T_0$ corresponds to complete disorder, i.e., $\psi_0 = 0.5$: 1) El'dzhurta granite cooling curve [5], horizontal axis time scale for crystals ~ 1 cm in size for various P_{H_2O}; 2) lines of equal degrees of order.

Ganguly pointed out [7]. If we wish to determine the state of the system of the moment when T during cooling has attained T_x, we can use the diagram if we represent the process as consisting of two stages (Fig. 3). Firstly, at the start ($\tau=0$, $\xi=\xi_0$), T falls instantaneously from T_0 to T_x (Fig. 3a), while ξ_0 remains unchanged. Secondly, under isothermal conditions at T_x, the reaction occurs in the interval τ_x-τ_0, which produces ξ_x (Fig. 3b). Let us step outside the *TTT* method and divide T_0-T_x into two parts: T -T_y and T_y-T_x, and represent the reaction in two stages (Fig. 3c). This means that initially the temperature fell instantaneously from T_0 to T_y, and in the first stage, the reaction occurred isothermally along the $\xi(T_y)$ curve for a time τ_y-τ_0 (Fig. 3d). Then at τ_y, there was a jump to a new stage with temperature T_x and another initial value of ξ_0, i.e., there is a shift to a new *TTT* diagram. At this degree, the reaction described by the $\xi(T_x)$ isotherm begins at the point corresponding to the state ξ_y and continues for a time τ_x-τ_y. The positions of the $\xi(T_x)$ and $\xi(T_y)$

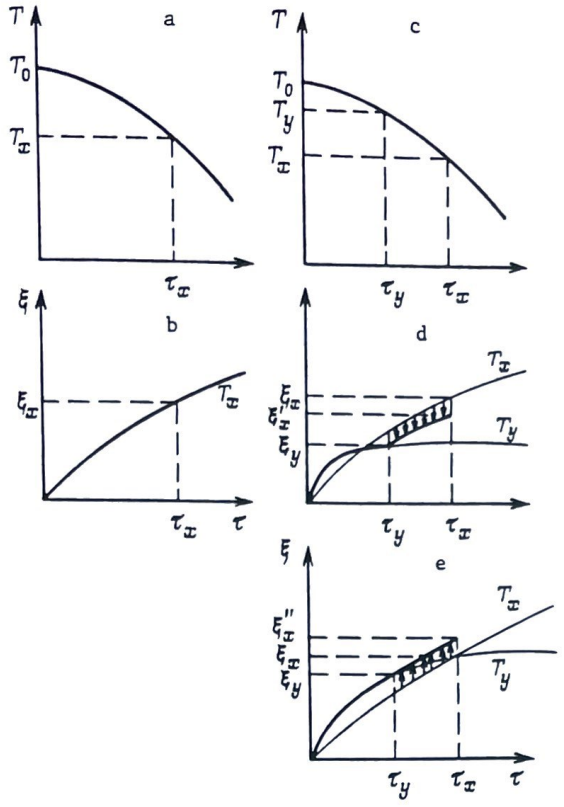

Fig. 3. One-stage and two-stage models for transformation during cooling: a) transformation along the cooling curve represented by the one-stage model; b) transformation isotherm corresponding to temperature T_x, with ξ_x the degree of conversion at time τ_x; c) two-stage model; d and e) differing degrees of conversion ξ_x' and ξ_x'' at time τ_x in two-stage model.

isotherms may result in reduction or increase in ξ_x' or ξ_x'' when τ_x is attained (Fig. 3d and e) by comparison with the single-stage model. If we increase the number of stages without limit, we will get the true value of ξ_x during continuous cooling. The essence of our method of estimating the conditions lies in passing from *TTT* diagrams to a kinetic equation of type (1) that is independent of the initial state. The division into infinitely small steps is provided during the computer solution. In order to avoid getting a curve with a turning point (as occurs in the *TTT* diagram method), which lacks physical significance the quenching conditions are estimated from the slowing-down in the change in ξ.

COOLING LAW

To analyze quenching conditions, we need to define the cooling rate as a function $T(\tau)$ and substitute for it into the kinetic equation relating the rate of change in ξ to the current values of ξ and T, which is then solved. In that approach, we neglect the heat effects of the transformation, which enables us to separate the kinetic problem from the thermal one; the latter can usually be handled by standard methods.

Consider a medium having a constant temperature T_*, into which we introduce an object with volume V and temperature $T_0 > T_\infty$. The temperature distribution at any instant can be derived from the conduction equation with the initial condition $T(x, 0) = T_0(x)$ and the boundary condition $T(\tau) = T_\infty$ (at the boundary of

volume V). A general solution can be obtained by separating the variables in the form of an infinite series [10]:

$$T(x, \tau) = T_\infty + (T_0 - T_\infty) \sum_{n=1}^{\infty} \frac{\int_V V_n(x)\, d^3x}{\int_V V_n^2(x)\, d^3x} V_n(x)\, e^{-\chi\lambda_n \tau}. \quad (2)$$

Here $T(x, \tau)$ is T at a point x at time τ, with χ the thermal diffusivity of the added body, while λ_n and $V_n(x)$, $n=1, 2, \ldots$ are determined uniquely by its geometry. For example, for a stratum with thickness l: $\lambda_n=(2n-1)^2\pi^2/l^2$, and $V_n(x)=\sin[(2n-1)\pi x/l]$. For a sphere with radius a: $\lambda_n=(n\pi/a)^2$, and $V_n(r)=\sin(\pi nr/a)$. For a cylinder with radius R: λ_n are the positive roots of $J_0(R, \lambda)=0$, in which J_0 is a Bessel function of the first kind and $V_n(r)=J_0(r, \lambda, n)$ [11]. It can be shown that the (2) series converges, and beginning at a certain time, the first nonzero term in (2) begins to predominate over the sum of the others. To examine differences in quenching conditions, thus we can compare the *TTT* method with the kinetic-equation one on the basis of a simplified cooling equation:

$$T(\tau) = T_\infty + (T_0 - T_\infty)\, e^{-K_c\tau}, \quad (3)$$

in which $K_c=\chi\lambda_1$ is a parameter with the dimensions of reciprocal time, which we subsequently call the cooling rate constant (for a stratum $K_c=\chi(\pi/l)^2$, for a sphere $K_c=\chi(\pi/a)^2$, and for a cylinder $K_c=\chi\lambda_1$, in which $\lambda_1=2.4/R^2$). At the same time, when we examine the zonation generated by uneven cooling, it is necessary to use the complete solution in (2).

EXPERIMENTAL DATA ON THE KINETICS OF INTRACRYSTALLINE TRANSFORMATIONS IN K-Na FELDSPARS

These general concepts may be illustrated in one of the fundamental petrologic systems: the alkali feldspar solid solutions, in which Al-Si ordering occurs. The behavior of the ordering during cooling is examined using experimental data [11-13] on the thermodynamics and kinetics of their transformations.

The alkali feldspars are represented in nature by monoclinic varieties — K and K-Na sanidines and orthoclases — and triclinic forms, which include the essentially potassic ordered microclines and sodian albites and the anorthoclases. The last are solid solutions enriched in the albite component, and they are monoclinic at the time of crystallization at high temperatures, but during cooling, they become triclinic as a result of a shearing transformation, while retaining their monoclinic topochemistry, i.e., the Al-Si distribution corresponding to sanidine [5]. To examine the thermal history of a rock on the basis of feldspar ordering, the most suitable varieties are intermediate and essentially disordered (in Al-Si distribution) varieties which have monoclinic topochemistry: sanidines and anorthoclases.

Al-Si ordering at constant temperature is [11, 13] described by a second-order kinetic equation:

$$\frac{d\psi}{d\tau} = -k(T, P_{H_2O}, l)\left[\frac{\psi(\tau) - \psi^*(T, P, x)}{\psi_0 - \psi^*(T, P, x)}\right]^2. \quad (4)$$

It is second order because it is necessary to fit the observed kinetic curves for small deviations from equilibrium. Here ψ characterizes the ordering. For monoclinic forms, $\psi \equiv 2t_1$, i.e., ψ corresponds to the proportion of Al atoms in the two T_1 positions per formula unit in the feldspar (K, Na)$AlSi_3O_8$ relative to the total amount (of one) in the four tetrahedral positions $2T_1 + 2T_2$ [14].

The ordering is catalyzed by water and probably involves a reaction front advancing within a grain, so we assume that the rate constant k should be dependent not only on T and P_{H_2O} but also on the effective grain size. There is

no evidence for an effect from the total pressure P, which suggests that the rate is independent of it. In accordance with [11, 13], we also assume that k here is independent of the composition X in the sanidine stability region.

The T dependence is defined by the measured activation energy of sanidine ordering E_a = 157.2 kJ/mol. The rate of ordering of sanidines as a function of P_{H_2O} is assumed to be the same as for albites, for which the rate is $\sqrt{P_{H_2O}}$ [15]. Data on sanidine ordering in experiments [11, 13] may be used with change in dimensions from h^{-1} to y^{-1} to get

$$k\,(\mathrm{yr}^{-1}) = 10^{8.41} P_{H_2O}^{0.5} \exp(-E_a/RT), \tag{5}$$

in which P_{H_2O} is in bar. The size of the experimental crystals was $\sim 10^{-2}$ mm. These data cannot be transferred directly to the real setting. To derive the ordering constant for natural crystals, we use the data given by Scott et al. [16], who calculated the cooling conditions in a layer of ignimbrites having a rhyolite-dacite composition in Nevada, and also derived the unit-cell parameters for the sanidines there. Those cooling conditions were calculated [16] by a standard method based on the error integral. An exponential law can be used to describe the cooling, as we have shown, and then (3) for the central part of the layer is

$$T(\tau,\ \mathrm{K}) = 298 + 755 \exp(-7{,}65 \cdot 10^{-4}\ \tau). \tag{6}$$

The initial cooling temperature was [16] 1023 K; the cooling rate constant was found to be K_c = 7.65 x 10^{-4} y^{-1}.

Using the unit-cell parameters with Luff's formulas [5], we estimated the state and composition of the sanidines from these Nevada ignimbrites which at the central part of the stratum had characteristics $2t_1$ = 0.59 and X = 0.72. One can simulate the potash feldspar ordering in the (6) mode of cooling and solve the inverse problem: from the cooling rate and the quenched degree of order, one gets k as

$$k = 10^{7.48} P_{H_2O}^{0.5} \exp(-E_a/RT). \tag{7}$$

We assume that P_{H_2O} was $\sim$ 100 bar and the crystal size $\sim$ 1 mm.

There are two sanidine generations in the El'dzhurta granite [5]: phenocrysts and groundmass. The groundmass crystals are also $\sim$ 1 mm in size, so we assumed that at the same T and P_{H_2O} they would order at the same rate as the KFs in the ignimbrites. Here $2t_1$ = 0.67 and the temperature at the start of cooling was T_0 = 1003 K, $P_{H_2O} \approx$ 1 kbar. Our method gave K_c = 1.26 x 10^{-5} y^{-1} in (3).

The sanidine phenocrysts evidently cooled in the same way as the groundmass. They are $\sim$ 1 cm in size, and $2t_1$ = 0.64. We derive k from them by simulating the conversion during cooling on the law derived for the El'dzhurta granites from the groundmass sanidines:

$$T(\tau,\ \mathrm{K}) = 298 + 705 \exp(-1{,}26 \cdot 10^{-5}\ \tau). \tag{8}$$

The quenching of the structural state found for the phenocrysts at P_{H_2O} 1000 bar is provided by the rate constant

$$k = 10^{6.71} P_{H_2O}^{0.5} \exp(-E_a/RT). \tag{9}$$

We thus have three estimates for k: (5), (7), and (9), whose differences we ascribe to the effective sizes of the synthetic and natural crystals. Subsequent calculations of the cooling rate from the degree of order have been done for rocks where we have observed or could assume that the crystals were $\sim$ 1 cm in size, i.e., we used the k corresponding to (9).

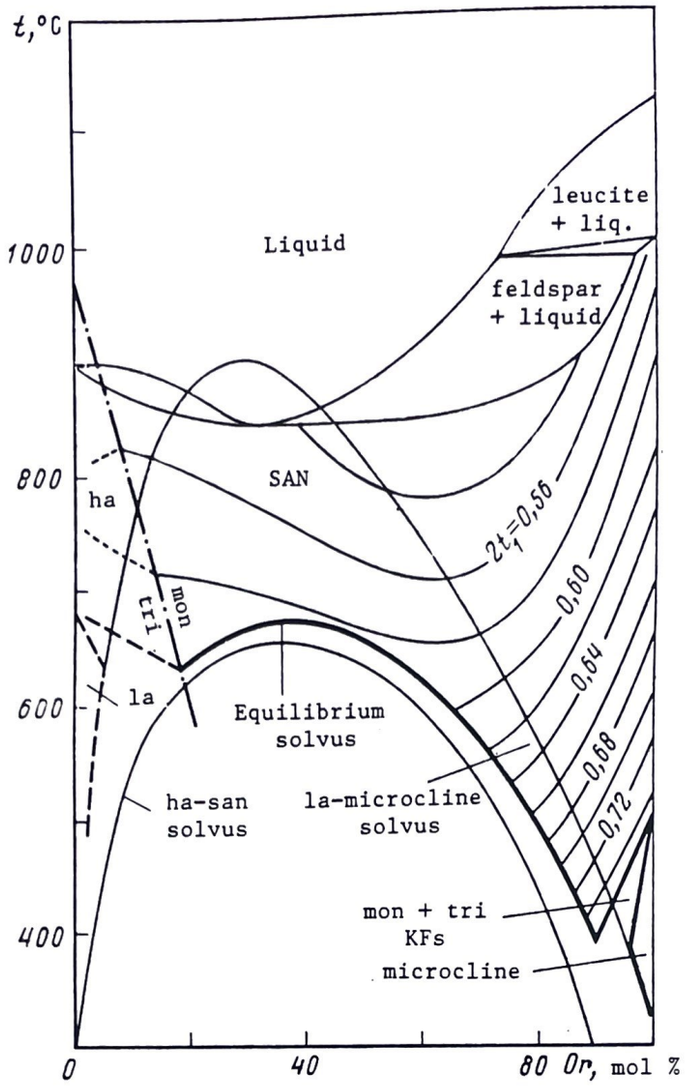

Fig. 4. Phase relationships in the $NaAlSi_3O_8$-$KAlSi_3O_8$ system at $P = P_{H_2O} = 1$ kbar [11, 12]. The sanidine solid-solution region SAN calibrated from degree of order $2t_1 \equiv \psi$; mon/tri, monoclinic-triclinic inversion line; ha, high albite; la, low albite.

The equilibrium $\psi^* \equiv 2t_1$ are shown in Fig. 4 as functions of T, P and X. They can be calculated from a formula for the positional distribution constant K_D derived from measurements as used in constructing Fig. 4 [11, 12]:

$$\ln K_D(T, P, x) = \ln \frac{\psi^*(1+\psi^*)}{(2-\psi^*)(1-\psi^*)} = (2.18X^3 - 2.7X^2 + 0.1X - 0.8) + (1996X^3 - 2777X^2 + 1885X + 981)\frac{1}{T} - p(0{,}009X^2 - 0{,}002X - 0.01)\frac{1}{T}. \quad (10)$$

In (10), T is in K, P is the total pressure in bar, and X is the molar fraction of $KAlSi_3O_8$ in the K-Na feldspar solid solution. The equation is applicable for $0.2 < X \leqslant 1$.

SIMULATING THE CHANGE IN ORDER DURING COOLING

In what follows we will examine two models based on different choices of the initial state ψ_0. In the first, it is assumed that the rock existed at T_0 for a time sufficient for the feldspar to attain equilibrium ψ at the start of

monotonal cooling at τ_0, and then ψ_0 in that state corresponded to equilibrium at T_0, i.e., $\psi_0 = \psi^*(T_0)$.

The second model involves a different assumption on the preparation of the initial state: the liquid precipitated completely disordered crystals, which were in equilibrium at a sufficiently high temperature or were formed as metastable phases. Synthesis experiments [13, 15, 17] indicate that disordered feldspars can crystallize at temperatures at which the disordered state does not correspond to equilibrium. The temperature T_0 at the start of slow cooling either coincides with the crystallization temperature or else the temperature reduction to T_0 (eruption) is sufficiently rapid for the initial disorder not to alter substantially during that preparative stage. Thus ψ_0 was taken as 0.5 in this model. In the standard *TTT* method, it is usually assumed that the initial state corresponds to complete disorder, although the method can be used with any choice for the initial state.

We used (4), (9) and (10) with various cooling rates obtained by varying T_0 and K_c in (3) to examine the ordering. We will assume in this that, by introducing the dependence of the coefficients in the isothermal kinetic equation on temperature, we can describe a nonisothermal process.

The numerical calculations were performed for T_0 of 1000-1400 K, K_c from 10^{-6} to 10^{-1} y^{-1}, P_{H_2O} 0.1-1 kbar, and various feldspar compositions X. P in accordance with (10) had very little effect on $\psi^*(T)$ in the range of several kbar. We also neglected how P affected the rate. We therefore neglected the role of P in the calculations and took it as 1 kbar.

Figure 5 shows the results for T_0 = 1000 K. For comparison, we have used contrasty conditions: K_c of 10^{-6} and 10^{-2} y^{-1}. We considered two models for the initial state: ψ_0 = 0.5 and $\psi_0 = \psi^*$(1000 K). The parameters $P = P_{H_2O}$ = 1 kbar and X = 0.7 were kept unchanged. For this composition, ψ^*(1000 K) = 0.557.

Along with the cooling curves (1) and the ordering curves (2a and 2b), Fig. 5 shows $\psi(\tau)$ curves with turning points (3a and 3b) that were derived by the *TTT* diagram method. Figure 5 also shows the equilibrium ψ (lines 4) on the $T(\tau)$ curves, which are the values that would be obtained if equilibrium were attained at each instant. The ψ_0 = 0.5 model leads to a discrepancy between the calculated and equilibrium values at the initial point.

The conversion curves obtained by numerical solution are continuous and do not have turning points, in contrast to the *TTT* ones. Thus determining the quenching parameters from them is in a certain sense nominal. Quenching was defined here as the instant when ψ passed through the point corresponding to 99% of the complete range between ψ_0 and ψ_∞, which on sufficiently prolonged cooling virtually ceased to change and corresponded to the flat parts of curves 2a and 2b in Fig. 5. The order at the instant of quenching is denoted by ψ_q. As all the ψ curves during cooling become very gently sloping as 300 K is approached, ψ_∞ on the flat part was determined as the value attained at that temperature: $\psi_\infty \approx \psi$(300 K), so $\psi_q = 0.99(\psi(300\ K) - \psi_0)$.

Figure 5, on which the instants of quenching are indicated, shows that the transformation persists throughout much of the cooling interval. The changes cease only when the rock has cooled to a few hundred degrees.

The differences between the two models for ψ_0 ought to decrease as T_0 increases because $\psi^*(T_0)$ tends to the value characterizing complete disorder. The differences vanish for X = 0.7 sanidine at T_0 = 1236 K, when the equilibrium value is ψ^*(1236 K) = 0.5. In accordance with this, the $\psi(\tau)$ curves for the different ψ_0 models come together as a single curve (Fig. 6).

Figure 6 also shows that with slower cooling (K_c 10^{-6} y^{-1}), the initial

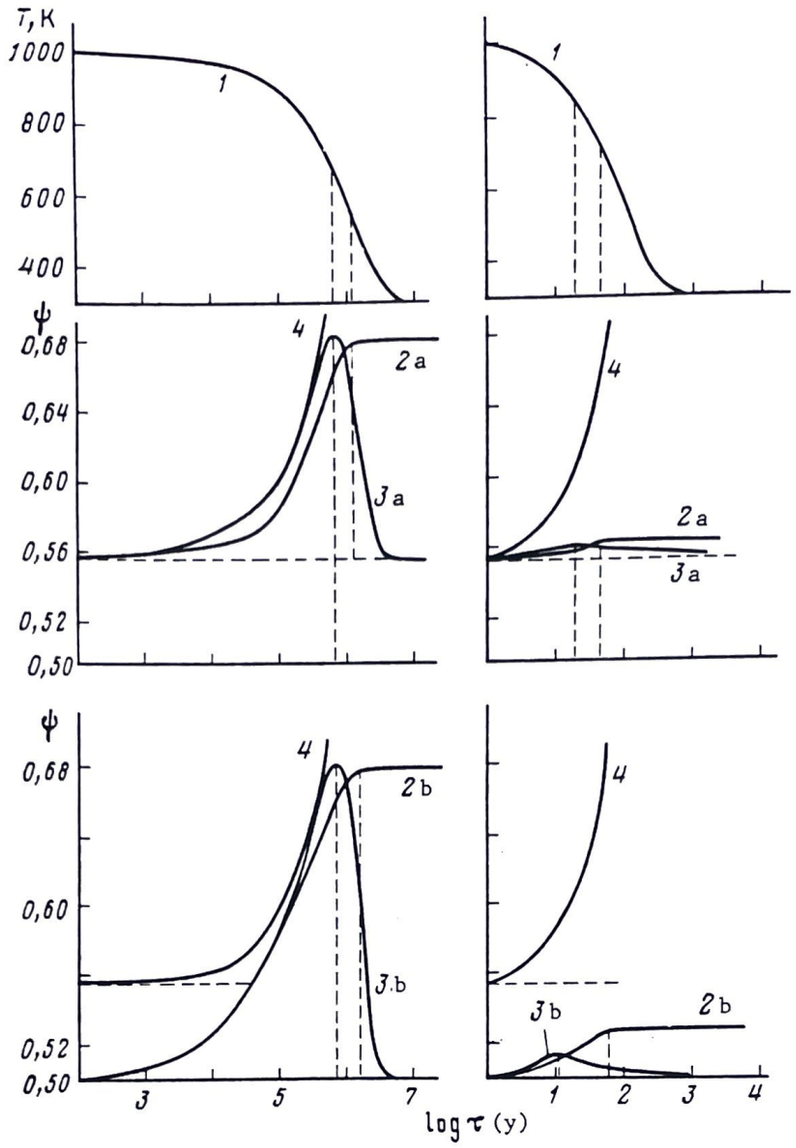

Fig. 5. Change in order on cooling from T_0 = 1000 K (P = P_{H_2O} = 1 kbar, X = 0.7). On the left, $K_c = 10^{-6}$; on the right, $K_c = 10^{-2}$ y^{-1}: 1) cooling curve; 2a and 2b) changes in order calculated numerically for ψ_0 = 0.5 (2b) and ψ_0 = ψ^*(1000 K) = 0.557 (2a); 3a and 3b) $\psi(\tau)$ from the *TTT* method (ψ_0 = ψ^*(1000 K) in 3a, ψ_0 = 0.5 in 3b); 4) equilibrium values along cooling curve. The vertical dashed lines indicate the instants of quenching from the numerical and *TTT* methods.

conditions are forgotten, and all the curves come together in the final stages, with quenching for slow cooling occurring under similar conditions in spite of the differences at the start. With rapid cooling, the calculated quenching state is dependent on the ψ_0 model.

EFFECTS OF THE QUENCHING STATE ON COOLING PARAMETERS

Figure 7 shows in more detail how ψ is dependent on the initial state. For $T_0 < 1236$ K, the lines do not coincide when the ψ_0 are taken differently. For practical purposes, one can assume that the differences vanish at about T = 1200 K.

Figure 8a gives the ψ_q derived numerically and from a *TTT* diagram. The case $T_0 \geqslant 1200$ K is shown, where the initial state is unimportant. The

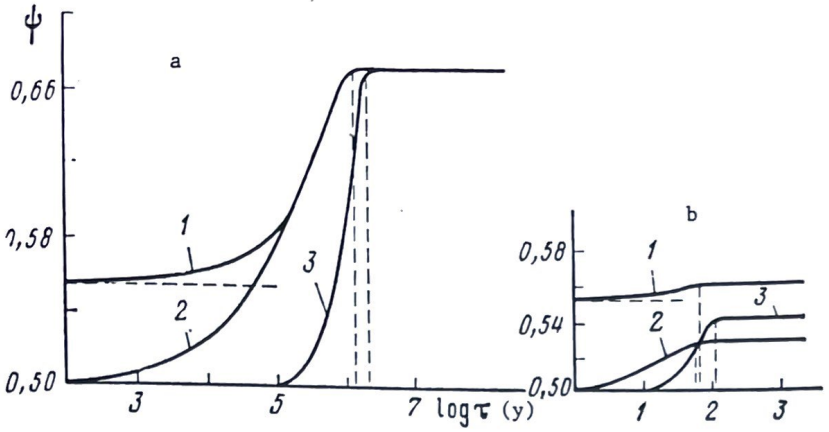

Fig. 6. Curves for $\psi(\tau)$ in sanidine (X = 0.7) at $P = P_{H_2O}$ = 1 kbar: a) $K_c = 10^{-6}$; b) $K_c = 10^{-2}$ y^{-1}. Lines: 1) T = 1000 K; ψ_0 = 0.557; 2) T_0 = 1000 K, ψ_0 = 0.500; 3) $T_0 \geqslant$ 1236 K.

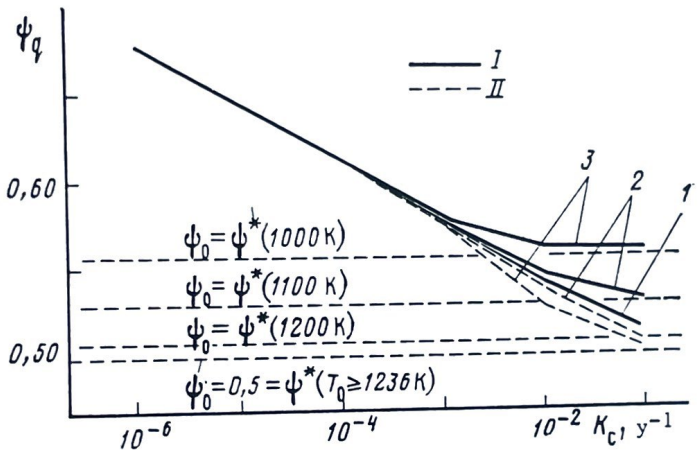

Fig. 7. Quenched degree of order ψ_q in sanidine specimens (X_{Or} = 0.7) in relation to cooling rate for various initial conditions. I) $\psi_0 = \psi^*(T_0)$; II) $T_0 \geqslant$ 0.5; 1) ψ_0 = 1200 K; 2) T_0 = 1100 K; 3) T_0 = 1000 K.

distances between lines 1 and 2 or 3 and 4 characterize the deviations in the real state frozen when the transformation is halted from the equilibrium one at the T and P of the halt. The more accurate numerical solution indicates a more marked difference between the quenched and equilibrium values than do the *TTT* estimates.

Figure 8b for $T_0 < 1000$ K indicates that the choice of ψ_0 influences the result for the halt state only for high cooling rates ($K_c \geqslant 10^3$ y^{-1}). The deviations from equilibrium remain much the same in all the forms of the calculations.

Parts c and d of Fig. 8 give estimates of the quenching temperatures for the nodes of cooling given in parts a and b of Fig. 8. Here we also show the temperature that would correspond to the system at the time of halt if one assumes that the ψ observed in the sanidine after the end of cooling is the equilibrium one at that moment. This is the apparent temperature of formation of the structural state of the feldspar $T^*(\psi\tau)$, which is substantially different

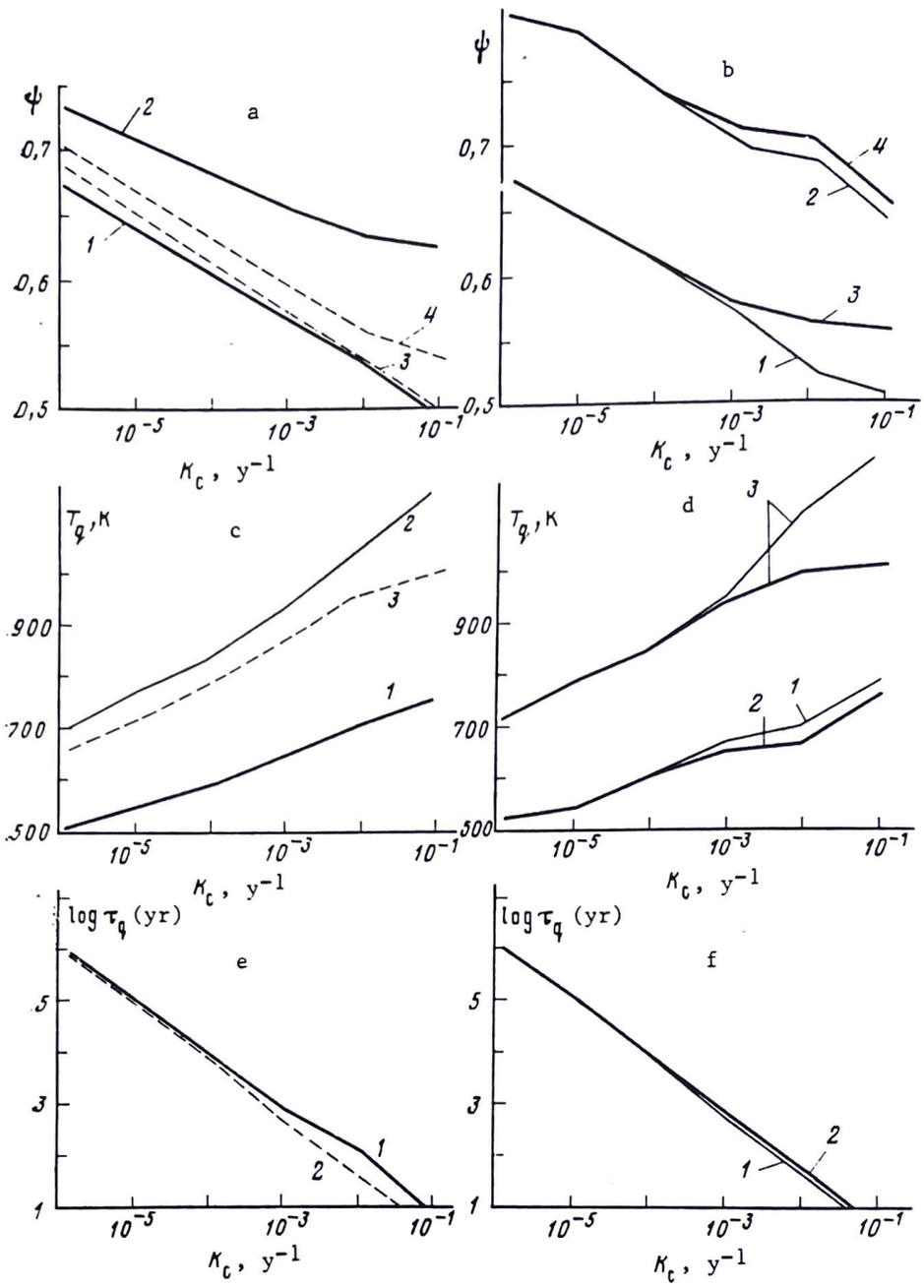

Fig. 8. Quenched and equilibrium degrees of order, the latter at the quenching temperatures, for various cooling rates ($P = P_{H_2O} = 1$ kbar, $X = 0.7$). a) $T_0 \gtrsim 1200$ K, 1) ψ_q derived numerically; 2) equilibrium values at quenching temperatures (numerically); 3) quenched values from *TTT* diagram; 4) equilibrium value at quenching temperature determined by *TTT* method; b) $T_0 = 1000$ K, lines 1 and 2 corresponding to $\psi_0 = 0.5$ and lines 3 and 4 to $\psi_0 = \psi^*(T_0)$. Quenching temperatures ($X = 0.7$, $P = P_{H_2O} = 1$ kbar): c) $T_0 \gtrsim 1200$ K, 1) numerical solution: 2) equilibrium temperature for sanidine with degree of order τ_q; 3) quenching temperature from *TTT* method; d) $T_0 = 1000$ K, 1) $\psi_0 = 0.5$; 2) $\psi_0 = \psi^*(1000\ K)$; 3) equilibrium temperatures for ψ_q derived from two models. Quenching times ($X = 0.7$, $P = P_{H_2O} = 1$ kbar); e) $T_0 \gtrsim 1200$ K, 1) numerical solution; 2) *TTT* diagrams; f) $T_0 = 1000$ K, 1) $\psi_0 = 0.5$; 2) $\psi_0 = \psi^*(1000\ K)$.

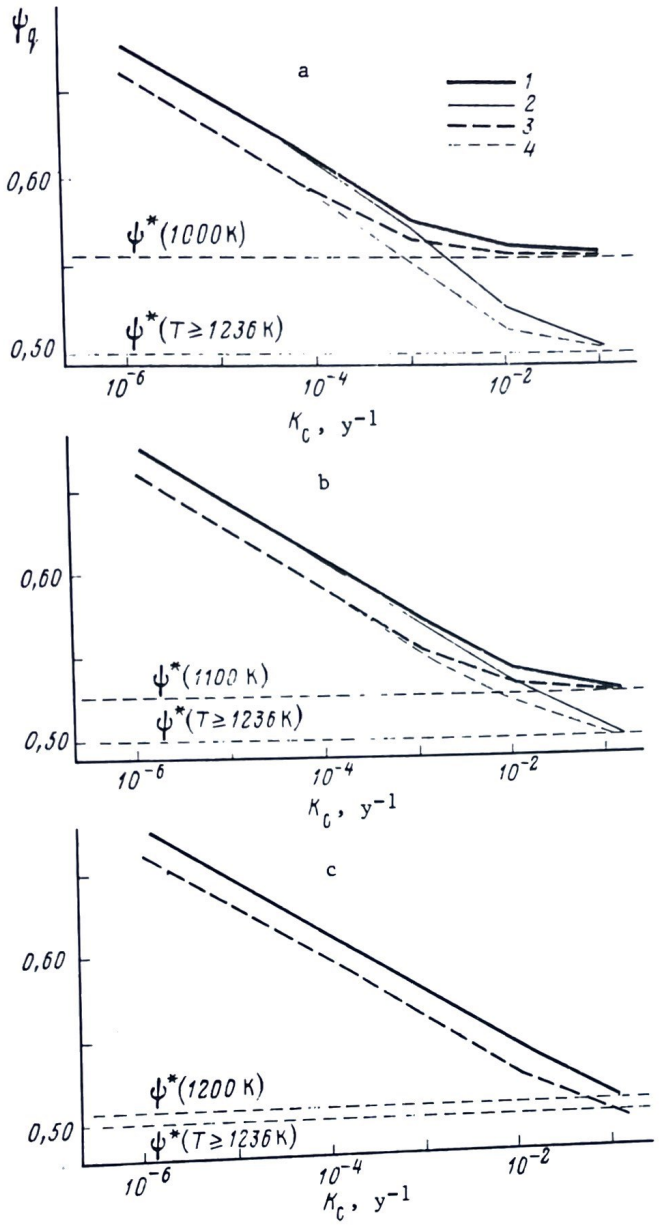

Fig. 9. Effects of water pressure on ψ_q for sanidine specimens with X = 0.7 and P_{tot} 1 kbar, P_{H_2O}: 1 and 2) 1 kbar; 3 and 4) 0.1 kbar; 1 and 3) ψ_0 = $\psi^*(T_0)$; 2 and 4) ψ_0 = 0.5; T_0: a) 1000 K; b) 1100 K; c) $\geqslant$ 1200 K.

from the actual quenching temperature. The direct use of sanidine ψ to estimate temperatures on the basis of equilibrium formation is thus erroneous.

Figure 8c shows that the quenching temperatures calculated numerically deviate appreciably from the *TTT* results, while Fig. 8d implies that the ψ_q and the quenching temperatures for the various ψ_0 models differ only at high cooling rates.

Parts e and f of Fig. 8 show calculations of the time τ_q-τ_0 during which changes occur in the feldspars as the rock cools. This period terminates at the instant of quenching and is called here the quenching time. The results obtained by the two methods do not differ substantially for the various ψ_0 models and differing T_0.

Figures 5-8 thus imply that numerical solution in general gives quenching parameter estimates that deviate more from the equilibrium values as regards temperature and ψ than do those from the less correct *TTT* method. The quenching parameters are determined primarily by the cooling rate, but at low initial temperatures ($T_0 < 1200$ K) and high cooling rates ($K_c \geq 10^{-3}$ y^{-1}), the estimates are also dependent on the choice of the initial state. If we assume that there was complete disorder in the Al-Si distribution at the start, the calculation leads to less ordered forms on quenching than in the case of an equilibrium initial value $\psi_0 = \psi^*(T_0)$.

As the ordering rate is dependent on P_{H_2O}, ψ_q decreases as the H_2O pressure falls. Figure 9 shows estimates of that parameter. The curves have been used to derive the thermal-history characteristics of certain feldspathic rocks by reference to the sanidine specimens.

Figure 9 shows that sanidine ordering data can be used correctly as a geochemical indicator only if P_{H_2O} is considered. For a given P_{H_2O}, sanidine (here with $X = 0.7$) gives an unambiguous indication of the cooling rate down to a state of order $\psi \approx 0.57$. If the disorder is even higher (0.57-0.50), the necessary branch in Figs. 7 and 9 can be derived only from additional information on the initial cooling temperature. It is sufficient to know whether the initial temperature range corresponds to $T_0 \geq 1200$ K, since all branches merge above that temperature, or if T_0 falls in the lower range, where one needs to make a more detailed examination of the estimates for the parameter. In volcanic and subvolcanic rocks that can be characterized by examining the sanidines, the condition $T_0 \geq 1200$ K appears to be met in most cases.

CONCLUSIONS

A method has been devised for examining the conditions of quenching of mineral transformations during continuous cooling, which is based on solving the kinetic equations together with the cooling ones. The method has been used to examine the conditions of quenching of K-Na feldspars. The basis is provided by experimentally established trends in the equilibrium ordering of the feldspars in relation to T, P and X together with data from kinetic research. The quenched degree of conversion (at a certain temperature) may differ considerably from the equilibrium one at that temperature. The method is found to have advantages over the *TTT* diagram one.

Feldspar ordering can be used as a geospeedometer, since it is dependent mainly on the cooling rate. Reliable results are not obtained in estimating the temperatures of origin of the rocks.

REFERENCES

1. Müller, R. and S. Saxena, 1980. Chemical Petrology [Russian translation], Mir, Moscow.
2. Patnis, A. and J. McConnell, 1983. Major Features of Mineral Behavior [Russian translation], Mir, Moscow.
3. 1981. Kinetics of Geochemical Processes. Reviews in Mineralogy, Miner. Soc. Amer., v. 8.
4. Groot, S. and P. Mazur, 1964. Nonequilibrium Thermodynamics [Russian translation], Mir, Moscow.
5. Khitarov, N. I., E. E. Senderov, A. M. Bychkov, et al., 1980. Osobennosti usloviy stanovleniya El'dzhurtinskogo granitnogo massiva [Conditions of Emplacement of the El'dzhurta Granite Intrusion], Nauka, Moscow.
6. Seifert, F. A. and D. Virgo, 1975. Science, v. 188, 1107.
7. Ganguly, J., 1982. Advances in Physical Geochemistry, v. 2, Springer-Verlag, New York, p. 58.
8. Saxena, S. K., 1983. Ibid., v. 3, p. 61.
9. Skogby, H., 1987. Phys. Chem. Miner., v. 14, No. 6, 521.
10. Carslaw, G. and D. Jäger, 1964. Thermal Conductivity of Solids [Russian translation], Nauka, Moscow.
11. Senderov, E. E., 1985. Subsolidusnyye fazovyye otnosheniya karkasnykh

alyumosilikatov [Subsolidus Phase Relationships of the Framework Aluminosilicates: D. Sc. Thesis], GEOKhI AN SSSR, Moscow.
12. Senderov, E. E., 1988. Tr. XI Vsesoyuz. soveshch. po eksperimental'noy mineralogii [Proceedings of the 11th All-Union Conference on Experimental Mineralogy], Nauka, Moscow, p. 21.
13. Bychkov, A. M., N. S. Vasil'yev, I. G. Vorob'yeva and E. E. Senderov, 1988. Tr. XI Vsesoyuz. soveshch. po eksperimental'noy mineralogii [Proceedings of the 11th All-Union Conference on Experimental Mineralogy], Nauka, Moscow, p. 125.
14. Kroll, H., 1971. Neues Jahrb. Miner. Monats., p. 91.
15. McConnell, J. D. C. and D. McKie, 1960. Miner. Mag., v. 32, No. 36.
16. Scott, R. B., S. W. Bachinsky, R. W. Nesbitt and M. R. Scott, 1971. Amer. Miner., v. 56, 1208.
17. Shchekina, T. N., E. E. Senderov, A. M. Bychkov and K. N. Tobelko, 1973. Geokhimiya, No. 1, 35.